CERN-INTC-2016-007 / INTC-P-457
11/01/2016

EUROPEAN ORGANIZATION FOR NUCLEAR RESEARCH

Proposal to the ISOLDE and Neutron Time-of-Flight Committee

Decay study of the onset of deformation in the ($A \sim 100$, $N = 60$) region by β-decay of ^{97}Kr

January 11, 2016

C. Sotty[1], C.R. Niţă[1], A. Algora[2], A. Andreyev[3], D.L. Balabanski[4], G. Benzoni[5], M.J.G. Borge[6], D. Bucurescu[1], C. Costache[1], D. Cullen[7], D.T. Doherty[3], P. Van Duppen[8], L.M. Fraile[9], G. Georgiev[10], M. Huyse[8], L.J. Harkness-Brennan[11], A. Ionescu[1], K. Johnston[6], D.T. Joss[11], D.S. Judson[11], S. Kisyov[1,12], J. Konki[13], U. Köster[14], A. Kusoğlu[15], S. Leoni[5], R. Lică[1,6], N. Mărginean[1], R. Mărginean[1], M. Madurga[6], C. Mihai[1], R.E. Mihai[1], E. Nacher[16], A. Negreţ[1], R.D. Page[11], S. Pascu[1], N. Pietralla[17], A. Şerban[1], L. Stan[1], T. Stora[6], A. Stuchbery[18], O. Tengblad[16], A.E. Turturică[1], V. Vedia[9], M. Zielinska[19], N. Warr[20], H. De Witte[8]

[1] *Horia Hulubei National Institute for Physics and Nuclear Engineering, Bucharest-Măgurele, Romania*
[2] *Instituto de Fisica Corpuscular, Univ. Valencia, Correos 22085, E-46071 Valencia, Spain*
[3] *University of York, Heslington, York YO10 5DD, United Kingdom*
[4] *ELI-NP, IFIN-HH, 30 Reactorului Street, 077125 Bucharest, Măgurele, Romania*
[5] *Dipartimento di Fisica, University of Milano, Milano, Italy and INFN, Sezione di Milano, Milano Italy*
[6] *ISOLDE, CERN, CH-1211 Geneva 23, Switzerland*
[7] *School of Physics and Astronomy, University of Manchester, Manchester, M13 9PL, United Kingdom*
[8] *KU Leuven, Instituut voor Kern- en Stralingsfysica, Celestijnenlaan 200 D, 3001 Leuven, Belgium*
[9] *Grupo de Física Nuclear,Facultad de CC. Físicas,Universidad Complutense, CEI Moncloa, 28040 Madrid, Spain*
[10] *CSNSM Orsay, 101 Domaine de l'Université de Paris Sud, 91400 Orsay, France*
[11] *Oliver Lodge Laboratory, The University of Liverpool, Liverpool, L69 7ZE, United Kingdom*
[12] *Faculty of Physics, University of Sofia "St. Kliment Ohridski", 5 Bld. James Bourcher, 1164 Sofia, Bulgaria*
[13] *Department of Physics, University of Jyväskylä, Jyväskylä FIN-40014, Finland*
[14] *Institute of Laue-Langevin, BP 156, 6, Rue Jules Horowitz, 38042 Grenoble, Cedex 9, France*
[15] *University of Istanbul, Beyazit, 34452 Fatih/Istanbul, Turkey*
[16] *Instituto de Estructura de la Materia, CSIC, Serrano 113 bis, E-28006 Madrid, Spain*
[17] *Institut für Kernphysik, TU Darmstadt, Darmstadt, Germany*
[18] *Department of Nuclear Physics, RSPE, Australian National University, Canberra, 2601, Australia*
[19] *CEA Saclay, L'Orme des Merisiers, 91191 Gif-sur-Yvette, France*
[20] *Institut für Kernphysik, Universität zu Köln, Köln, Germany*

(IDS Collaboration)

Co-Spokesperson: C. Sotty [*Christophe.Sotty@cern.ch*], C.R. Niţă [*crnita@tandem.nipne.ro*]
Contact person: R. Lică [*Razvan.Lica@cern.ch*]

Abstract:

Recent isomeric decay studies from ILL and RIKEN have identified the presence of an isomeric state lying at 76.5 keV ($T_{1/2}$=5.7(6)μs) above the ground state of the ^{97}Rb isotope, situated at the border of the onset of deformation in the ($A \sim 100$, $N = 60$) region. Proposed as a shape isomer, the character of this state needs to be established. Further Coulomb excitation studies confirmed the $\pi g_{9/2}[431]3/2^+$ Nilsson orbital as the g.s. rotational band configuration of $^{97}Rb_{60}$. Most of the matrix elements have been determined except for the 68-keV state. Our proposal aims to perform a detailed spectroscopy study of ^{97}Kr using the recently commissioned ISOLDE Decay Station (IDS): by means of lifetime, decay and electron spectroscopy measurements in order to determine the β-feeding, the multipole mixing ratios and the matrix elements, which will infer information on the shape transition. The experimental data will allow to distinguish between the single-particle and more collective (deformed) character and will constitute a benchmark to guide the nuclear models that describe the shape transition in this region of the nuclear chart.

Requested shifts: [46] shifts, (split into [2] runs over [2] years)
[24] shifts, for the decay spectroscopy and fast-timing run
[22] shifts, for the electron spectroscopy run

1 The Region of Deformation around A∼100, N=60

1.1 Current knowledge

Similar to the rare earth, the ($A \sim 100$, $N = 60$) region has already been studied due to the presence of one of the most sudden onset of deformation. Since its discovery via fission [1], considerable efforts have been made to understand it [2, 3, 4]. β-decay studies of mass separated fragments from induced and spontaneous fission provided the identification of the lowest states of rotational bands characteristic of deformed structures for Z=37-42 nuclei ($\beta \sim 0.3-0.4$) along the isotopic chains [5, 6, 7, 8, 9, 10, 11, 12, 13]. In this part of the chart of nuclides, the systematics of the measured electric quadrupole and magnetic dipole moments [14], charge radii of the ground states, as well as the energies of the first 2_1^+ and 4_1^+ states and their related transition decay strengths in even-even nuclei, point towards the existence of a shape transition. However, more experimental studies are required to evidence and characterize the single-particle like states in odd mass nuclei in the nearby mass region.

The strongest development of deformation is seen in the Sr and Zr isotopic chains at $N \sim 60$. On the proton side, the shape transition starts to be smoother for the Kr [15] and Mo isotopes. For the latter, the fact that the deformation decreases, has been tentatively explained for $Z > 37$ by possible appearance of triaxiality [16, 17, 18, 19]. The Kr isotopes are the first showing a smooth development of deformation indicated by the systematics of the S_{2n}, $E(2_1^+)$, $R_{4/2}$ and $B(E2, 2_1^+ \rightarrow 0_1^+)$ observables [15, 20, 21, 22], which implies that the Rb isotopic chain is the first exhibiting a strong development while increasing the proton number. As expected, the phenomenon of shape coexistence at low excitation energy manifests in intermediate cases at $N \sim 60$ [4, 23, 24, 25, 26, 27, 28], such as for the ^{96}Rb or ^{97}Sr, for which shape isomers have already been measured.

The shell model calculations suggested that the iso-vector interaction between the $\pi g_{9/2}$ and $\nu h_{11/2}$ particles for the Zr isotopes has been considered to have an important role in the appearance of deformation [29, 30]. However, we could consider of low importance the influence of the $\nu h_{11/2}$ intruder orbitals at the onset of deformation [31]. The $\nu h_{11/2}$ orbit starts to play a dominant role for larger neutron number. According to deformed mean field calculations [17, 32, 33, 34], the deformation driving components of the $\nu h_{11/2}$ intruder orbit lie below the Fermi level at $N \sim 60$. The low-Ω orbital from the $\nu h_{11/2}$ are in this picture preferably occupied compared to the $\nu g_{7/2}$ orbitals. By analogy with the rare earth isotopes, the intruder orbitals are expected to stabilize the deformation, as done in the rare earth nuclei by the intruder orbitals arising from the $\nu i_{13/2}$ orbit.

The identification of the origin of the isomeric states constitutes a piece of the puzzle to understand the mechanisms involved in the development of deformation for which the $\nu h_{11/2}$ and the filling of the $\pi g_{9/2}$ play a preponderant role. For example, nearby the Rb isotopes, the character of the isomeric states can be most likely interpreted as originating from multiparticle configurations involving the $\nu h_{11/2}$ and most likely the $\nu g_{7/2}$ and/or the $\pi g_{9/2}$. Recent isomeric decay studies of ^{97}Rb by Kameda [35] (RIKEN) and Rudigier [36] (ILL) revealed the presence of a shape isomer ($T_{1/2}$=5.7(6)μs) in the ^{97}Rb, identified thanks to γ-ray (E1) transition of 76.5 keV feeding directly the ground state. Comparisons between HFB and QPRM calculations lead to a spin/parity assignment of $(1/2, 3/2)^-$; however, several orbitals can be assigned to this isomeric state, the low-lying prolate $3/2^-[312]$ or oblate $1/2^-[321]$, $3/2^-[321]$ quasiparticle excitations [36].

Further Coulomb excitation studies performed on ^{97,99}Rb a REX-ISOLDE using the MiniBall setup revealed a rotational-like structure built on top of the ground state [37]. The ground state Nilsson configuration has been firmly established to be $\pi_{9/2}[431]3/2^+$. For the ^{97}Rb isotope, most of the matrix elements have been determined except for the first excited state lying at 68 keV above the ground state. In both nuclei, the low-lying states decaying onto the ground state have potentially long lifetimes ($\sim$ hundreds ps). This conclusion was drawn from what has been observed within the Coulex analysis applying Doppler corrections on different flight path components.

The understanding of the complex mechanisms involved in the appearance of deformation and shape isomers in the ($A \sim 100$, $N = 60$) region requires to perform further experimental studies. One proposes

to investigate the region by performing a detailed spectroscopy study of the odd mass ^{97}Rb isotope populated via the ^{97}Kr β-decay using the recently commissioned ISOLDE Decay Station (IDS). Due to continuous developments of its target and ion source performances, ISOLDE is the only facility able to produce very intense neutron-rich Kr beams whose decay can be studied. The ISOLDE Decay Station is a permanent experimental setup which allows to perform complete spectroscopy of implanted RIB nuclei. The close geometry, combined with using very good energy and time resolution detectors for highly efficient γ-ray detection, fast β plastics and neutron detectors makes it an unique and versatile setup also taking into consideration the future plans to install a conversion electron spectroscopy array which is under design.

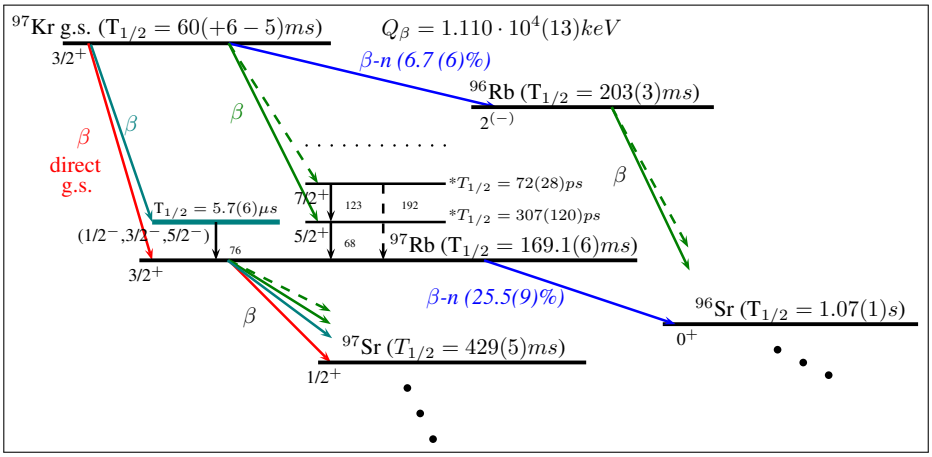

Figure 1: Subsequent decay chain resulting from ^{97}Kr. The scheme is based on the Coulomb excitation [37] and isomeric decay [35, 36] spectroscopic studies. The evaluated $\beta - n$ branches and g.s. half-lives values are taken from Ref. [38, 39]. The half-lives with an asterisk are estimated from the B(M1) and B(E2) values from Ref. [37].

1.2 Experimental Goals

The ^{97}Kr β decay is a unique case, since placed at the shape transition it might populate well-deformed, single-particle-like structures or resulting from multiparticle configurations or isomeric states, which would decay for some of the states with low energy γ transitions implying high electronic conversion. In addition, thanks to other selection rules than the previous measurements, the β decay might populate unobserved states belonging to those different single particle like or more collective structures. The evolution of the preferential feedings and energy position of each structure is crucial to clearly disentangle the mechanisms involved in the sudden development of deformation.

An independent and direct determination of the lifetimes, conversion coefficients and mixing ratios will bring consistency in the determination of the matrix elements. Moreover, it would validate the protocol used to extract the matrix elements from Ref. [37], which relied on calculated values such as for the conversion coefficients [40], the Alaga rules. The detailed spectroscopy study of the ^{97}Kr β decay is proposed to be performed in two independent runs with two different experimental configurations: the first one is dedicated to the decay spectroscopy study and lifetime measurements using the Fast-Electronic Timing Technique, and, the second aims to perform an electron spectroscopy study.

Decay Spectroscopy & Lifetime Measurements by Fast-Electronic Timing Technique
The ground state of the ^{97}Kr nucleus is assumed to have $J^\pi = 5/2^+, 3/2^+$ [41]. According to the selection rules, several excited states of the ^{97}Rb should be populated via β decay, e.g. with $J^\pi = 5/2^+, 3/2^+$ ($\Delta J = 0, 1$, for allowed Fermi and Gamow-Teller) [42]. It is also expected to populate with a certain hindrance the related states with $\Delta J > 1$ [27].

Benefiting from a large Q_β-value ($1.110 \times 10^4(13)$keV), the β decay might populate several states with $J^\pi = 3/2^+, 5/2^+, 7/2^+$ located at high excitation energy, above the neutron separation, which decay by γ cascades to the g.s. and possibly onto the lowlying states already identified in the previous studies.

Some of the populated states may be based on the $[440]1/2^+$ configuration which mixes with the g.s. band [37]. These new states would decay by emitting γ-rays which are unknown. To investigate the γ-spectroscopy of ^{97}Rb, β-γ, β-γ-γ, γ-γ coincidence studies will be used. Such discovery would help to understand the evolution of each configurations promoting deformed Nilsson configuration while increasing the number of proton/neutron. The extraction of the β direct feeding to the g.s. will be based on previous β- and β-n decay studies of ^{97}Kr [43].

We would like to measure for the first time the lifetimes of the $5/2^+$ and $7/2^+$ states belonging to the deformed band based onto $\pi_{9/2}[431]3/2^+$(g.s.) in ^{97}Rb. The multipolarity of the γ transitions linking the well deformed band states are of pure M1/E2($\Delta I = 1$) or E2($\Delta I = 2$) character. Values of the mixing ratio can be inferred from the reduced transition probabilities presented in Ref. [37], except for the first excited state lying at 68 keV.

The feasibility of using the fast-timing technique to measure these lifetimes is presented below.

Estimations of expected lifetimes:
Since there is no experimental multipole mixing ratio available for the mixed [M1+E2] 68-keV or 123-keV transitions, a value of $\delta(E2/M1)$ was deduced from the M1 and E2 transition probabilities presented in Ref. [37] for the 123-keV transition ($7/2^+ \rightarrow 5/2^+$) in ^{97}Rb. For intraband M1+E2 ($J^+ \rightarrow (J-1)^+$) transitions, the mixing ratio is given by: $\delta^2(E2/M1) \propto E_2^5/E_1^3 \cdot B(E2)/B(M1)$. The extracted values from the Coulomb excitation experiment [37], are B(M1)=0.28(11) μ_N^2 and B(E2)=0.33(+11-14) $\times$ $10^4 e^2 fm^4$ and combined determine a magnitude of $\delta(E2/M1)$=0.11(3) which further give for the $7/2^+$ state an expected lifetime of τ = 104(40) ps. For the 68-keV ($5/2^+$) state, a mixing of $\delta(E2/M1)$=0.11(3) results in a lifetime value of τ = 430(169) ps, taking into consideration also the internal conversion competing process (α_{tot}=0.468(7) [40]).

All the estimated lifetimes are within the range of the fast-timing technique. Considering that the time distribution will be obtained using β-γ coincidences, the prompt response function measured with this detector configuration (as during IS590 performed in 2015) using a ^{60}Co source would give for the TAC(β-$LaBr_3$) spectrum a time resolution of FWHM$\sim$240 ps. Although, β-$LaBr_3$(1)-$LaBr_3$(2) events are highly unlikely to be used due to the poor expected statistics, the measured time resolution for the TAC(γ-γ) using the same source run was FWHM$\sim$150 ps for γ-ray energies $E_\gamma \approx 1$ MeV (^{60}Co source). An estimation of the absolute statistical error on the measured lifetime is about 5% or better depending on the statistics. Therefore, the centroid shift or the slope methods may be used to extract the lifetime from the final time distributions. During the proposed experiment on-line sources will be used.

The experimental setup:
For this analysis, will be used with the existing IDS experimental setup consisting of 1 fast plastic scintillator, 2 $LaBr_3$(Ce) detectors (conical crystals with 1.0“ $\times$ 1.5“) and 4 clovers HPGe are available (at least 3 mounted), see Fig. 2. Two HPGe planar detectors are available in case we would like to optimize the efficiency at low energies (at least one will be mounted). The acquisition will be run in triggerless mode. The time intervals between the population of a state and its direct decay are recorded with Time to Amplitude Converter (TAC) modules between the beta plastic and the $LaBr_3$(Ce) detectors. Therefore, data will be sorted in $E_\gamma(LaBr_3)$-$\Delta T(T_\beta - T_\gamma)$ structures with an a priori condition to select only the coincidences with the β radiation. The "start" signal is given by the β (feeding) radiation, while the "stop" signal that closes the TAC gate is the γ-ray that signals the direct decay of the state of interest. Additional gate selections (e.g. on the time since proton impact) may be applied before obtaining the final energy spectra or time distributions, details of different conditions are contained in Tab. 1.

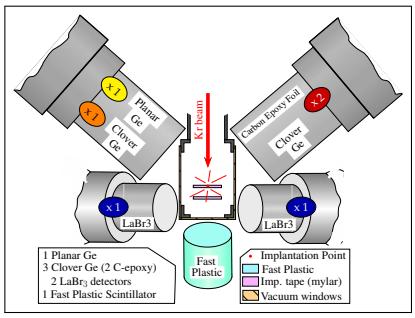

Figure 2: Decay Spectroscopy/Lifetime setup.

Energy [keV]	ϵ_{HPGe}	ϵ_{LaBr_3}	β-γ_{LaBr_3} [Cts] /20 shifts	β-γ_{HPGe} [Cts] /20 shifts
68	0.08	0.04	7700	15500
123	0.14	0.07	6500	13000
103	0.14	0.08	8000	14000
192	0.10	0.06	400	700
227	0.08	0.06	6000	8000
76.5	0.08	0.04	4000	8000

Table 1: Decay Spectroscopy/Lifetime setup. Expected counting rates in β-gated single spectra ^{97}Kr (g.s.) β-decay. Due to the energy similarity of the 68- and 76-keV transitions, an additional selections can be used, such as gating onto the feeding γ transition on the 68-keV state. The estimated counting rate for β-γ(HPGe;124 keV)-γ(LaBr$_3$;68 keV)(t) is of about 1200 counts, without any time gate applied.

Off-line calibration sources will be used to remove the amplitude dependence of the timing signal induced by the electronics (e.g. by the constant fraction discriminators used in the block diagram to trigger the TAC modules) between the fast β plastic and each of the LaBr$_3$(Ce) detectors. Also, the prompt coincidences may be used to perform the alignment of the timing signals. The on-line data runs will be used, before starting the actual analysis, to check the walk-correction.

Estimations of the counting rates:
We assume a 1 μA proton beam and a transmission of 50% from primary target to tape station. Yields from the primary target are taken from the last ISOLTRAP campaign (2015, ^{97}Kr beam). The implantation yield has been determined to be 200 pps. The β-feeding of the excited states have been all taken as 1% and the branching ratios for the $7/2^+$ (g.s. rotational band) decay have been taken from the Coulomb excitation [37]. The β efficiency has been measured experimentally to be 12%. The Germanium and LaBr$_3$(Ce) γ-ray efficiencies have been determined using the same experimental setup. The $\beta - n$ branch considered in the calculations represents the adopted value [38]. In order to clean the dataset from the different contaminations or contributions from the subsequent decay products, see Fig. 1, a gate on the time since proton impact has to be set and this will reduce the statistics by around one half. Moreover, the tape station would be turned every 2.0 seconds after the proton impact, which imposes to request of no consecutive proton pulses. Thus, an average value of 30% of the proton pulses on our target from the super cycle was considered. The expected yields are summarized in Table 1. Also, for the 68-keV state lifetime, β-LaBr$_3$ coincident events can be selected with an additional gate imposed onto the 123-keV populating transition in the HPGe detectors. This further gives a statistics lower by more than an order of magnitude in the final time distribution, of about 1200 events. If the proton gate is applied then only one-half of the statistics remains, about 600 events in the time distribution.

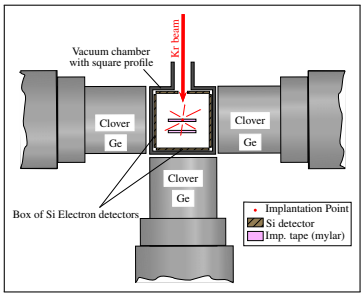

Figure 3: Electron Spectroscopy setup.

Energy [keV]	BR(CE)	Si Counts
68	0.6875	172000
76.5	0.1770	44400
123	0.2063	52000

Table 2: Electron Spectroscopy setup. Expected counting rates in the Si spectra ^{97}Kr (g.s.) β-decay. The BR(CE) are deduced from BrIcc [40].

Electron Spectroscopy
In order to determine properly the matrix elements notably within the g.s. band, the complementary measurement of the electronic conversion coefficients is necessary to deduce the multipole mixing ratio which would refine the precision of the matrix elements. One propose to perform an electron spectroscopy

study of the different states populated by the ^{97}Kr β-decay. The beam characteristics and the number of shifts are similar to what has been taken for the decay spectroscopy study when estimating the counting rates.

For the conversion electron spectroscopy measurements, several possible detection configurations are proposed. An experimental setup consisting of 3 HPGe (2 with C-epoxy foil) and a Si box($\epsilon_{Si} \sim 0.3$) may be envisaged, see Fig. 3. The HPGe detectors would be employed to filter the dataset selecting only a given decay cascade. The Si box consists of DSSDs placed around the implantation point. One high request when measuring conversion electrons is represented by the energy resolution, which is expected to be as good as a few keV which is enough to resolve our conversion peaks. This setup can also be improved by replacing the Si box, if this expectation is not fulfilled, with 2 LN_2-cooled Si(Li) detectors with expected better energy resolution. It is also foreseen a new design of the frame, with the forward angles restricted for γ detection. Simulations will be performed for each configuration to establish the most efficient configuration of the final setup.

A large background coming from the β and γ-ray emissions enforces to acquire a large statistics to be able to extract with a sufficient precision the mixing ratios from the electronic conversion coefficients. The estimated counting rates are given in Tab. 2 for the configuration given in Fig. 3.

Target and Contamination:
The Kr isotopes are produced with a UC_x target, using a plasma ion source with cooled transfer line (VADIS source). From the 2015 ISOLTRAP campaign (UC541-VD7), the yield of ^{97}Kr was 2000 ions/s with a current of 1 μA. The main contaminants ($\sim$ 90%) was coming from doubly-charged $A = 194$ isobars (Tl, Pb, Hg, Au) most likely ^{194}Hg. In order to minimize the possible isobaric/doubly-charged contaminations, we would like to employ the HRS separator and possibly the neutron converter. As performed during the last ISOLTRAP Kr run, the target settings have to be tuned in order to optimize the Kr/contamination ratio and test if it is worth to use the neutron converter. Most probably, it would be mandatory to use the latter for the electron spectroscopy in order to reduce the background in the Si detectors (which do not suffer of low intrinsic efficiencies). Such tests have been realized using the IDS setup during the last IS590 run (^{68}Mn).

Summary of requested shifts: [46] shifts, (split into [2] runs over [2] years)

[**24**] shifts, for the **decay spectroscopy and fast timing run** (out of which 2 shifts are dedicated to acquire time calibration data with on-line sources, 1 shift to tune the target settings, 1 shift to validate our experimental setup with a less exotic case)

[**22**] shifts, for the **electron spectroscopy run** (out of which 1 shift is dedicated to tune the target settings, 1 shift to validate our experimental setup with a less exotic case)

References

[1] S.A.E. Johansson. *NP*, (64):p. 147–160, 1965.
[2] M.A.C. Hotchkis *et al. NP*, A(530):p. 111–134, 1991.
[3] E. Cheifetz *et al. PRL*, 25:38–43, Jul 1970.
[4] R.A. Meyer ed. J. Eberth and K. Sistemich, editors. Bad Honnef, Springer, Berlin, 1988, 1988.
[5] E. Monnand *et al. Z. Phys. A*, 306:183–184, 1982.
[6] F.K. Wohn *et al. PRL*, 51:873–876, Sep. 1983.
[7] K. Shizuma *et al. Z. Phys. A*, 315:65–75, 1984.
[8] T. Seo *et al. Z. Phys. A*, 320:393–398, 1985.
[9] B. Pfeiffer *et al. Z. Phys. A*, 317:123–124, 1984.
[10] T. Seo *et al. Z. Phys. A*, 315:251–253, 1984.
[11] R.A. Meyer *et al. NPA*, 439(3):510–534, 1985.
[12] R.F. Petry *et al. PRC*, 31:621–633, Feb 1985.
[13] R.F. Petry *et al. PRC*, 37:2704–2721, Jun 1988.
[14] N.J. Stone. *Atomic Data and Nuclear Data Tables*, 90(1):75–176, 2005.
[15] M. Albers *et al. PRL*, 108:062701, Feb 2012.
[16] A.G. Smith *et al. PRL*, 77:1711–1714, Aug. 1996.

[17] P. Bonche, H. Flocard, P.H. Heenen, S.J. Krieger and M.S. Weiss. *NPA*, 443(1):39–63, 1985.
[18] H. Hua *et al. PRC*, 69:014317, Jan. 2004.
[19] R. Rodríguez-Guzmán *et al. PLB*, 691(202), 2010.
[20] S. Naimi *et al. PRL*, 2010.
[21] N. Mărginean *et al. PRC*, 80:021301, Aug. 2009.
[22] V. Manea *et al. PRC*, 88:054322, Nov 2013.
[23] H. Mach *et al. PLB*, 21, 1989.
[24] J.A. Pinston *et al. PRC*, 71:064327, Jun. 2005.
[25] G. Lhersonneau *et al. Z. Phys. A*, 330:347–348, 1988.
[26] W. Urban *et al. NPA*, 689(3):605–630, 2001.
[27] G. Lhersonneau *et al. Z. Phys. A*, 337:149–159, 1990.
[28] M. Büscher *et al. PRC*, 41:1115–1125, Mar 1990.
[29] P. Federman and S. Pittel. *PLB*, 69(4):385–388, 1977.
[30] P. Federman and S. Pittel. *PRC*, 20:820–829, Aug. 1979.
[31] A. Etchegoyen *et al. PRC*, 39:1130–1133, Mar. 1989.
[32] A. Faessler *et al. NPA*, 230(2):302–316, 1974.
[33] D. Galeriu *et al. Journal of Physics G: Nuclear Physics*, 12(4):329, 1986.
[34] A. Kumar and M.R. Gunye. *PRC*, 32:2116–2121, Dec 1985.
[35] D. Kameda *et al. PRC*, 86:054319, Nov 2012.
[36] M. Rudigier *et al. PRC*, 87:064317, Jun 2013.
[37] C. Sotty *et al. PRL*, 115:172501, Oct 2015.
[38] N. Nica. *Nuclear Data Sheets*, 111, 525, November 2009.
[39] A.A. Sonzogni D. Abriola. *Nuclear Data Sheets*, 109, 2501, 2008.
[40] T. Kibédi *et al.* BrIcc v2.3S Conversion Coefficient Calculator, 21 Dec. 2011.
[41] G. Audi, A.H. Wapstra, and C. Thibault.
[42] J. Suhonen. *From Nucleons to Nucleus.* Springer-Verlag, 2007.
[43] U.C. Bergmann *et al. NPA*, 714(1-2):21–43, 2003.

Appendix

DESCRIPTION OF THE PROPOSED EXPERIMENT
The experimental setup comprises: (*name the fixed-ISOLDE installations, as well as flexible elements of the experiment*)

Part of the	Availability	Design and manufacturing
(if relevant, name fixed ISOLDE installation: COLLAPS, CRIS, ISOLTRAP, MINIBALL + only CD, MINIBALL + T-REX, NICOLE, SSP-GLM chamber, SSP-GHM chamber, or WITCH)	☒ Existing	☒ To be used without any modification
[Part 1 of experiment/ equipment]	☐ Existing	☐ To be used without any modification ☐ To be modified
	☐ New	☐ Standard equipment supplied by a manufacturer ☐ CERN/collaboration responsible for the design and/or manufacturing
[Part 2 of experiment/ equipment]	☐ Existing	☐ To be used without any modification ☐ To be modified
	☐ New	☐ Standard equipment supplied by a manufacturer ☐ CERN/collaboration responsible for the design and/or manufacturing
[insert lines if needed]		

HAZARDS GENERATED BY THE EXPERIMENT (if using fixed installation:) Hazards named in the document relevant for the fixed [COLLAPS, CRIS, ISOLTRAP, MINIBALL + only CD, MINIBALL + T-REX, NICOLE, SSP-GLM chamber, SSP-GHM chamber, or WITCH] installation.

Additional hazards:

Hazards	[Part 1 of experiment/ equipment]	[Part 2 of experiment/ equipment]	[Part 3 of experiment/ equipment]
Thermodynamic and fluidic			
Pressure	[pressure][Bar], [volume][l]		
Vacuum			
Temperature	[temperature] [K]		
Heat transfer			
Thermal properties of materials			
Cryogenic fluid	[fluid], [pressure][Bar], [volume][l]		
Electrical and electromagnetic			
Electricity	[voltage] [V], [current][A]		
Static electricity			
Magnetic field	[magnetic field] [T]		
Batteries	☐		
Capacitors	☐		
Ionizing radiation			
Target material [material]			
Beam particle type (e, p, ions, etc)			
Beam intensity			
Beam energy			
Cooling liquids	[liquid]		

Gases	[gas]		
Calibration sources:	□		
• Open source	□		
• Sealed source	□ [ISO standard]		
• Isotope			
• Activity			
Use of activated material:			
• Description	□		
• Dose rate on contact and in 10 cm distance	[dose][mSV]		
• Isotope			
• Activity			
Non-ionizing radiation			
Laser			
UV light			
Microwaves (300MHz-30 GHz)			
Radiofrequency (1-300 MHz)			
Chemical			
Toxic	[chemical agent], [quantity]		
Harmful	[chem. agent], [quant.]		
CMR (carcinogens, mutagens and substances toxic to reproduction)	[chem. agent], [quant.]		
Corrosive	[chem. agent], [quant.]		
Irritant	[chem. agent], [quant.]		
Flammable	[chem. agent], [quant.]		
Oxidizing	[chem. agent], [quant.]		
Explosiveness	[chem. agent], [quant.]		
Asphyxiant	[chem. agent], [quant.]		
Dangerous for the environment	[chem. agent], [quant.]		
Mechanical			
Physical impact or mechanical energy (moving parts)	[location]		
Mechanical properties (Sharp, rough, slippery)	[location]		
Vibration	[location]		
Vehicles and Means of Transport	[location]		
Noise			
Frequency	[frequency],[Hz]		
Intensity			
Physical			
Confined spaces	[location]		
High workplaces	[location]		
Access to high workplaces	[location]		
Obstructions in passageways	[location]		
Manual handling	[location]		
Poor ergonomics	[location]		

Hazard identification:

Average electrical power requirements (excluding fixed ISOLDE-installation mentioned above): [make a rough estimate of the total power consumption of the additional equipment used in the experiment]